

# Optically rewritable 3D liquid crystal displays

J. Sun, A. K. Srivastava,\* W. Zhang, L. Wang, V. G. Chigrinov, and H. S. Kwok

State Key Laboratory on Advanced Displays and Optoelectronics Technologies, Department of Electronic and Computer Engineering,  
Hong Kong University of Science and Technology, Clear Water Bay, Kowloon, Hong Kong, China

\*Corresponding author: abhishek\_srivastava\_lu@yahoo.co.in

Received August 5, 2014; accepted August 24, 2014;  
posted September 8, 2014 (Doc. ID 220365); published 0 MONTH 0000

Optically rewritable liquid crystal display (ORWLCD) is a concept based on the optically addressed bi-stable display that does not need any power to hold the image after being uploaded. Recently, the demand for the 3D image display has increased enormously. Several attempts have been made to achieve 3D image on the ORWLCD, but all of them involve high complexity for image processing on both hardware and software levels. In this article, we disclose a concept for the 3D-ORWLCD by dividing the given image in three parts with different optic axis. A quarter-wave plate is placed on the top of the ORWLCD to modify the emerging light from different domains of the image in different manner. Thereafter, polaroid glasses can be used to visualize the 3D image. The 3D image can be refreshed, on the 3D-ORWLCD, in one-step with proper ORWLCD printer and image processing, and therefore, with easy image refreshing and good image quality, such displays can be applied for many applications viz. 3D bi-stable display, security elements, etc. © 2014 Optical Society of America

OCIS codes: (120.2040) Displays; (220.1140) Alignment; (230.0230) Optical devices; (350.0350) Other areas of optics.  
<http://dx.doi.org/10.1364/OL.99.099999>

The 3D display technology is now becoming a new trend of the display industry. Huge amounts of money were invested in the development of a 3D display system with wide viewing angle, high resolution, free-viewing and excellent 3D image quality. The 3D image can be realized by two approaches: first, stereoscopic that includes 3D vision by means of active or passive goggles, and the second approach (i.e., auto-stereoscopic method) involves holograms or the projection of the two images directly in to the human eye through parallax barrier and lens array. The stereoscopic 3D displays, including color-multiplexed (anaglyph) displays, time-multiplexed displays, polarization-multiplexed displays, and location-multiplexed displays, provide different views to the left and right eye [1–5].

Stereoscopic 3D effects can be achieved by displaying the two different but related images with two different colors [3,4] or different polarization states [5] of light into the eyeglasses. Humans wearing the eyeglasses can see only one image in each eye, which is integrated by the human's brain to generate the 3D sense.

On the other hand, auto-stereoscopic displays use optical components to achieve the effect of having different images visible on the same plane from different points of view. The parallax barriers [6], parallax illumination, and lenticular sheets [7] were used to divide a display resolution between two or more views. The display must have a fixed pixel pitch to allow aligning the barrier or lenslets with the pixel structure [8].

Recently, a new kind of display has been developed that allows us to address the display panel by optical means [9]. Such displays, i.e., optically rewritable liquid crystals display (ORWLCD), include LC sandwiched between two glass substrates (without current conducting layer) coated with two different alignment layer, one of them being optically active while other is optically passive. Primarily the easy axis on both alignment layers are set to provide the planer alignment conditions. The optically passive alignment layer is insensitive to the light exposure, whereas the optically active alignment layer provides an opportunity to change its easy axis by the

exposure through the polarized light. Therefore, intensities of different pixels on the ORWLCD panel can be modulated, by the photo exposure, to display a different image as a whole [10]. Thereafter, the written image can be displayed without any power consumption.

Moreover, because of the huge demand of displays with 3D content, several efforts have been made to create the 3D images for the ORWLCD, but the 3D image on ORWLCD imposes many tight limitations. Reference [9] disclosed a method to display 3D content by deploying two ORWLCD panels. The left and right images have been uploaded on two different ORWLCD panels; afterward both of these panel have been placed one over the other to overlap both of these images. The image quality with acceptable crosstalk could be fine for some applications; however, it needs double cell to define the 3D images and also the two same images cannot be overlapped, which results in huge cross talk in the two images. Furthermore to refresh the image on such a 3D ORWLCD panel, one has to update left and right images separately and afterward overlap them precisely, which is a tedious, expensive and time-taking process.

In this article, we disclose a method to generate the 3D image on the ORWLCD panel in one step.

The whole panel has been divided in to three parts with different image appearance, i.e., one for the left eye, a second for the right eye and a third for the background and front of the image. The complete 3D image with a good light printer can be updated on the ORWLCD panel in one step and thereafter could be permanently stored without consuming any power. With the feasibility of one-step 3D image writing, wide viewing angles, high contrast and low power consumption, this technology is suitable for many applications.

The ORWLCD consists of two substrates with different aligning materials, one of which, after being exposed by polarized light, is optically passive (insensitive to light exposure) and keeps a fixed easy axis, whereas the other aligning layer is optically active and can change its easy axis. A sulfonic azo dye (SD1) (Dai-Nippon Ink and Chemicals, Japan) is used as the optically active

alignment layer. The exposure of the SD1 layer by the polarized light of wavelength ( $\lambda$ ) 450 nm provides the alignment in the direction perpendicular to the E-vector of the exposing light, with almost zero pretilt angle and high azimuthal anchoring energy. When the SD1 layer is irradiated by a polarized light, the energy absorbed by SD1 molecules is proportional to the square of the cosine  $\theta$ , where the angle  $\theta$  characterizes the orientation of dye molecule with respect to the polarization vector of exposing light [11]. In other words, the alignment mechanism can be described in terms of the probability distribution that is nonuniform and shows good angular dependence. Therefore, the azo-dye molecules that have their transition dipole moments parallel to the direction of the plane of polarization of the impinging light gets excess energy, which results in their reorientation from the initial position to the direction orthogonal to the plane of polarization of the impinging light. This process gives an excess of chromophores in a direction where the absorption oscillator is perpendicular to the plane of the polarization of the impinging light. Thus the exposure of the SD1 substrate by the polarized light of wavelength ( $\lambda$ ) 450 nm provides the alignment direction (i.e., easy axis) perpendicular to the plane of polarization of the impinging light with almost zero pretilt angle and high anchoring energy. The anchoring energy of SD1 layer increases with the irradiation energy and saturates at higher energy. Moreover, the easy axis of the SD1 layer can be changed by another exposure through the polarized light of the same  $\lambda$  but a different polarization azimuth [12].

The ORWLCD cell with optically active and passive alignment layers has been prepared by coating the 0.5% solution of SD1 in N, N dimethylformamide (DMF) for the optically active substrate. The optically passive layer can be made of any photo-insensitive alignment material (either PI or photo alignment). In the present case, we have chosen 2% solution of PI 3744 that was coated as the optically passive alignment layer. The cell thickness was maintained at 10  $\mu\text{m}$  to maintain the waveguide regime of the ORWLCD panel. Thereafter, the cell has been filed with the LC of selected parameters. The selected parameters include elastic constant, viscosity, isotropic transition temperature, etc. [10].

The schematic diagram of the ORWLCD panel has been shown in the Fig. 1. The basic principle of the ORWLCD panel involves the switching between the planer and twisted nematic electro-optical mode [12,13]. First, both the substrate of the ORWLCD panel has been set to provide the planer alignment. The optical active layer (i.e., SD1) of the cell has been irradiated through the mask with the polarized light having a specific plane of polarization in order to provide SD1 alignment orthogonal, in-plane, to the previous direction. Therefore, after the second irradiation, the easy axis under the exposer window re-orient in the orthogonal direction with respect to the covered region, in the substrate plane. Thus the irradiated area represents the twisted alignment region, and non-irradiated area remains in the planer alignment regime and therefore can be distinguished under the crossed polarizers [14].

Figure 2 represents the optical microphotograph for the ORWLCD panel with two domains (i.e., with mutually perpendicular easy axis for the optically-active alignment

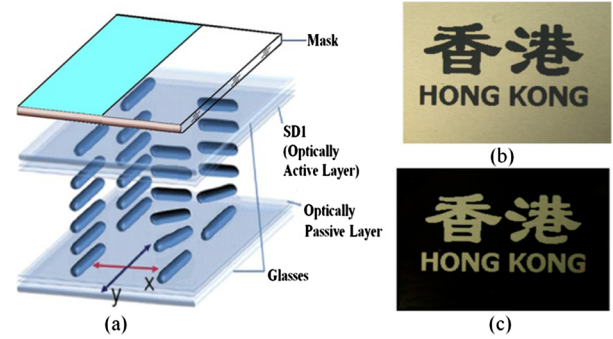


Fig. 1. (a) Schematics of the ORWLCD panel where the two alignment domain with PA and TN doiman can be created after the irradiation by polarized light ( $\lambda = 450$  nm). The covered domain shows PA, while the open area presents the transformed TN domian. (b) and (c) represent the images of the ORWLCD cell in parallel and crossed polarizers, respectively. The black region in (b) and white region in (c) represents the TN doiman.

layer) under the crossed polarizer. The uniform alignment and good anchoring energy of the alignment layer are two critical parameters for a good optical appearance of the image on an ORWLCD panel. If the alignment is not uniform, it will show some defects; on the other hand, weak anchoring energy results in low effective twist angle and thus the poor optical contrast ratio. Thus it is important to have good uniformity and azimuthal anchoring energy. The uniformity of the alignment is clear from Figs. 1(b), 1(c), and 2. In addition to that, the azimuthal anchoring energy provided by the azo-dye SD1 is  $\sim 1 \times 10^{-4}$  J/m<sup>2</sup>, which is sufficient to achieve the desired twist angle and thus the distinct gray scale [10–16].

A concept to display stereoscopic 3D image on the ORWLCD includes creation of the multiple domains with different twist angles. Such a stereoscopic 3D image contains three broad domains followed by multiple sub-domains. The concept is based on the generation of two opposite handedly circularly polarized light for the two different images for left and right eye of the observer. In this respect, two domains with twist angle  $+45^\circ$  and  $-45^\circ$ , with respect to the easy axis of the optically passive alignment layer, have been created. Thus the light passing through these domains followed by quarter wave plate (QWP) becomes right-handed circularly polarized (RCPL) and left-handed circularly polarized light (LCPL) that can be discriminated by the Polaroid.

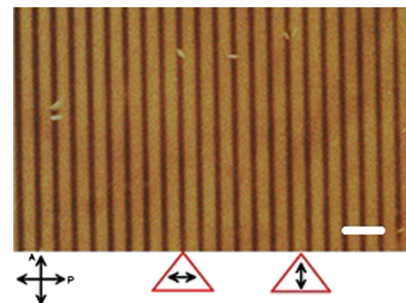


Fig. 2. Optical micrograph of the ORWLCD Cell with two alignment domains in crossed polarizers. The dark domain with the horizontal arrow shows PA domain, while the vertical arrow shows the TN domain. The white marker is equal to 100  $\mu\text{m}$ .

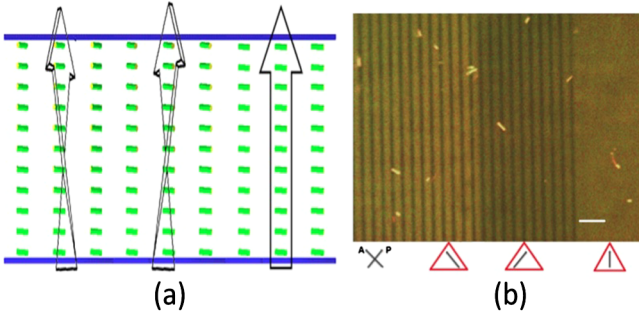


Fig. 3. (a) Schematic diagram for the 3D ORWLCD display with three alignment domains, first with  $+45^\circ$  twist and second with  $-45^\circ$  and third with  $0^\circ$  twist, i.e., PA. The corresponding optical micrograph has been shown in (b), the arrows orientation shows the polarization azimuth in different alignment domains. The white marker is equal to  $200\ \mu\text{m}$ .

Figure 3(a) shows the schematic of the optics for the 3D ORWLCD panel.

To generate the 3D image sense on the ORWLCD panel, the whole panel is divided in to three alignment domains with twist angle  $+45^\circ$ ,  $-45^\circ$  and  $0^\circ$  with respect to the easy axis of the optically passive alignment layer, respectively. Thereafter, a QWP with optical axis parallel to the easy axis of the domain with  $0^\circ$  twist angle has been placed on the top of the ORWLCD panel. Because of the waveguide regime, the light coming out from the cell follows the twist of the easy axis on the top layer. The incident light in terms of jones matrix can be written as

$$\vec{E}_{\text{in}} = \begin{bmatrix} \cos \theta \\ \sin \theta \end{bmatrix}, \quad (1)$$

where  $\theta$  is the angle between the polarization of incident light and x-axis. The QWP can be defined as

$$\vec{T} = \begin{pmatrix} 1 & 0 \\ 0 & \exp\left(-i\frac{\pi}{2}\right) \end{pmatrix}. \quad (2)$$

Thus after passing through the QWP, the output light takes the form

$$\vec{E}_{\text{out}} = \begin{pmatrix} 1 & 0 \\ 0 & \exp\left(-i\frac{\pi}{2}\right) \end{pmatrix} \begin{bmatrix} \cos \theta \\ \sin \theta \end{bmatrix} = \begin{bmatrix} \cos \theta \\ -i \sin \theta \end{bmatrix}. \quad (3)$$

When  $\theta = \pi/4$ ,  $-\pi/4$  and  $0$ , the output light is  $\frac{1}{\sqrt{2}} \begin{bmatrix} 1 \\ -i \end{bmatrix}$  (i.e. LCPL),  $\frac{1}{\sqrt{2}} \begin{bmatrix} 1 \\ i \end{bmatrix}$  (i.e. RCPL),  $\begin{bmatrix} 1 \\ 0 \end{bmatrix}$  (i.e., linearly polarized light), respectively.

Thus the light coming out of the first domain (i.e., with  $+45^\circ$  of twist angle) after passing through the QWP turns in to the LCPL, and light coming out of the second domain (i.e., with  $-45^\circ$  of twist angle) after passing through QWP turns into the RCPL; however, the light from the third domain (i.e., with twist angle =  $0^\circ$ ) does not have any effect of QWP and preserves the linearly polarization state. The microscopic optical texture of the three domains with three different twist angles is shown in Fig. 3(b). Thus in association with the good rewritability of the easy axis of the optically active azo dye SD1, with high resolution down to a few nanometer, one can achieve

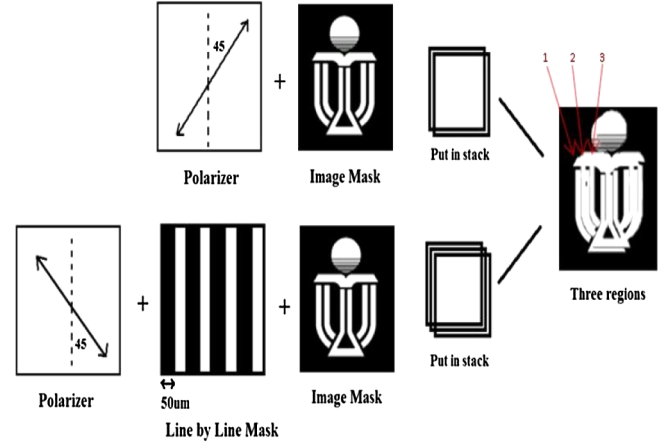


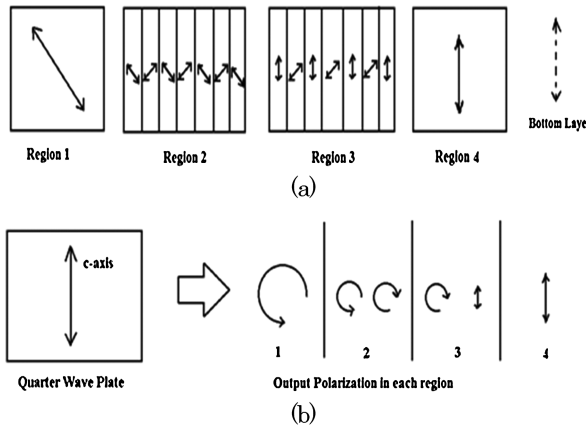
Fig. 4. Schematic diagram to illustrate the fabrication of three alignment domains in simple steps by irradiation, first without mask, second with image mask and  $+45^\circ$  of polarization azimuth and third with the amplitude mask with  $100\ \mu\text{m}$  period underneath of the image mask and polarization azimuth  $-45^\circ$ .

multiple alignment domains with different twist angles [17].

After proving the concept and limitation theoretically, the real 3D image has been realized for the ORWLCD panel. The schematic of the 3D image has been shown in Fig. 4. As illustrated earlier that the 3D image on the ORWLCD panel has to be divided in multiple domain with three different twist angles, the image has been realized by three-step irradiation. First, the ORWLCD panel has been set to provide  $0^\circ$  twist angle in respect of the bottom alignment layer (i.e., optically passive alignment layer); thereafter in the second step, the ORWLCD panel has been irradiated through the right image mask by polarized light with polarization azimuth at  $+45^\circ$  with respect to the first irradiation. The second step generates the right eye image. Afterward, in the third step, the same ORWLCD panel has been irradiated through the periodic amplitude mask (with period of  $100\ \mu\text{m}$ ), stacked with the left image mask, by the polarized light with polarization azimuth orthogonal to the second step. Consequently, the easy axis of the area underneath the open window re-orient orthogonally to the easy axis by the second exposure. Thus we obtained the multiple domains with three different twist angles. Moreover, the 3D depth can be controlled by controlling the shift in the left and right images.

The director profile in each domain has been illustrated in Fig. 5(a). The dotted arrow shows the easy axis on the bottom substrate, while arrows in regions 1, 2, 3 and 4 represent the relative twist angle in different domains. A QWP has been placed just after the ORWLCD panel with its optical axis aligned parallel to the easy axis of the bottom substrate (i.e.,  $0^\circ$  twist angle). The polarization states of the light in different region, after passing through the QWP, have been shown in Fig. 5(b). Thus by using the polarides, we can distinguish two regions, with twist angle  $+45^\circ$  and  $-45^\circ$ , separately for the left and right eye, whereas light passing through the domain with twist angle  $0^\circ$  will be visible from both eyes.

With the same concept, a 3D image for Hong and Chinese character 香 has been developed and shown in



F5:1 Fig. 5. (a) Represents the output polarization azimuth of the  
 F5:2 light from the three regions. (b) represents the polarization  
 F5:3 azimuth of the light from the three regions after passing a  
 F5:4 QWP on the top of the ORWLCD cell.

263 Fig. 6. Figure 6(a) shows the image for the left eye while  
 264 Fig. 6(b) shows the image for the right eye. Thus two different  
 265 images for different eyes offer the 3D image  
 266 scenes. Another important issue in displaying the 3D  
 267 images is crosstalk that depends on many parameters viz.  
 268 how well the image is separated, quality of the amplitude  
 269 mask (which is used for the third exposure), how well it  
 270 is restricted, and the polarizer quality. To optimize the  
 271 crosstalk, several periodic masks with different periods  
 272 have been studied and found that the mask with periodicity  
 273 of 100  $\mu\text{m}$  provides best optical quality with crosstalk  
 274 less than 6.5%. For the mask with smaller period, the  
 275 optical quality decreases because of several other limita-  
 276 tions related to the anchoring energy and alignment  
 277 layer, diffraction, and dispersion, etc. [14] the disclina-  
 278 tion line between the two domains is another issue for  
 279 the crosstalk that depends on the anchoring energy  
 280 and the LC cell gap. In the chosen conditions and align-  
 281 ment layer, it is restricted well below 10  $\mu\text{m}$ , which is be-  
 282 yond the human eye resolving power for such displays;  
 283 therefore, it is not the concern for the proposed  
 284 ORWLCD panel [11,17].

285 In summary, a method for generating 3D image on Op-  
 286 tically Rewritable LCD (ORW LCD) is presented. By mak-  
 287 ing use of the photo-alignment, the two same but  
 288 overlapping images (word “Hong” and “香” in Chinese)  
 289 are optically written on the cell with a slight position  
 290 shift (for the 3D depth) and different alignment configura-  
 291 tion. For the experimental demonstration, three irradiation  
 292 steps have been used; however, with proper high-resolu-  
 293 tion light printer and proper image processing, one can  
 294 address the ORWLCD panel in one step to upload the 3D  
 295 image [18]. Furthermore, the proposed 3D-ORWLCD is  
 296 bi-stable and does not require any power to hold the im-  
 297 age once it is optically uploaded; therefore, such displays



(a) (b)  
 Fig. 6. Two different pictures for different eyes taken from  
 different polarizers on the stereoscopic goggles. [two movies  
 are attached to show the effect for different eye (Media. 1)  
 and the display (Media. 2)]

can find applications in various modern display, security  
 and photonic devices.

Funding from partners State Key Laboratory on  
 Advanced Displays and Optoelectronics Technologies,  
 Hong Kong University of Science and Technology, Hong  
 Kong.

## References

1. S. Pastoor and M. Wopking, *Displays* **17**, 100 (1997). 305
2. I. Sexton and P. Surman, *Signal Process. Mag.* **16**(3), 85 306  
1999. 307
3. A. J. Woods and C. R. Harris, *Proc. SPIE* **7253**, 0Q1 (2010). 308
4. A. K. Srivastava, J. L. B. Tocnaye, and L. Dupont, *J. Disp. 309  
Technol.* **6**, 522 (2010). 310
5. S. Fans, *Proc. SPIE* **2177**, 180 (1994). 311
6. Y. H. Tao, Q. H. Wang, J. Gu, W. X. Zhao, and D. H. Li, *Opt. 312  
Lett.* **34**, 3220 (2009). 313
7. W. X. Zhao, Q. H. Wang, A. H. Wang, and D. H. Li, *Opt. Lett.* 314  
**35**, 4127 (2010). 315
8. N. A. Dodgson, *Computers and Society* **8**, 32 (2005). 316
9. A. Muravsky, A. Murauski, V. Chigrinov, and H. S. KWOK, 317  
*Jpn. J. Appl. Phys.* **47**, 6347 (2008). 318
10. J. Sun, A. K. Srivastava, L. Wang, V. G. Chigrinov, and H. S. 319  
Kwok, *Opt. Lett.* **38**, 2342 (2013). 320
11. V. Chigrinov, V. Kozenkov, and H. S. Kwok, “*Photoalign- 321  
ment of Liquid Crystalline Materials: Physics and Appli- 322  
cations*,” (Wiley, 2008), p. 248. 323
12. J. Sun and V. G. Chigrinov, *Mol. Cryst. Liq. Cryst.* **561**, 1 324  
(2012). 325
13. Y. Ma, J. Sun, A. K. Srivastava, Q. Guo, V. G. Chigrinov, and 326  
H. S. Kwok, *Europhys. Lett.* **102**, 24005 (2013). 327
14. V. Chigrinov, S. Pikin, A. Verevochnikov, V. Kozenkov, M. 328  
Khazimullin, J. Ho, D. D. Huang, and H. S. Kwok, *Phys. Rev. 329  
E* **69**, 061713 (2004). 330
15. A. D. Kiselev, V. G. Chigrinov, and H. S. Kwok, *Phys. Rev. E* 331  
**80**, 011706 (2009). 332
16. A. K. Srivastava, W. Hu, V. G. Chigrinov, A. D. Kiselev, and **1** 333  
Y. Q. Lu, *Appl. Phys. Lett.* **101**, 031112 (2012). 334
17. E. A. Shteyner, A. K. Srivastava, V. G. Chigrinov, H. S. Kwok, 335  
and A. D. Afanasyev, *Soft Mater.* **9**, 5160 (2013). 336
18. Y. Qiang, A. Murauski, T. Du, L. Yao, V. Chigrinov, and H. S. **2** 337  
Kwok, *Sid Digest Technol. Papers* **XL**, I-III, 1184 (2009). 338

## Queries

1. AU: A check of online databases revealed a possible error in this reference. The volume has been changed from '100' to '101'. Please confirm this is correct.
2. AU: Please check all the info in Ref. [18] for correctness and update the changes if any.